# $(NEt_4)_2[Fe(CN)_2(CO)('S_3')]$: An Iron Thiolate Complex Modeling the $[Fe(CN)_2(CO)(S{-}Cys)_2]$ Site of [NiFe] Hydrogenase Centers**

**Dieter Sellmann,* Franz Geipel, and Frank W. Heinemann[a]**

*Dedicated to Professor Lothar Beyer on the occasion of his 65th birthday*

**Abstract:** In the search for complexes modeling the $[Fe(CN)_2(CO)(cysteinate)_2]$ cores of the active centers of [NiFe] hydrogenases, the complex $(NEt_4)_2[Fe(CN)_2(CO)('S_3')]$ (**4**) was found ($'S_3'^{2-}$ = bis(2-mercaptophenyl)-sulfide(2−)). Starting complex for the synthesis of **4** was $[Fe(CO)_2('S_3')]_2$ (**1**). Complex **1** formed from $[Fe(CO)_3$-(PhCH=CHCOMe)] and neutral $'S_3'{-}H_2$. Reactions of **1** with $PCy_3$ or DPPE (1,2-bis(diphenylphosphino)-ethane) yielded diastereoselectively $[Fe(CO)_2(PCy_3)('S_3')]$ (**2**) and [Fe(CO)-(dppe)('$S_3'$)] (**3**). The diastereoselective formation of **2** and **3** is rationalized by the *trans* influence of the $'S_3'^{2-}$ thiolate and thioether S atoms which act as π donors and π acceptors, respectively. The *trans* influence of the $'S_3'^{2-}$ sulfur donors also rationalizes the diastereoselective formation of the $C_1$ symmetrical anion of **4**, when **1** is treated with four equivalents of $NEt_4CN$. The molecular structures of **1**, **3**·0.5 $C_7H_8$, and $(AsPh_4)_2[Fe(CN)_2(CO)('S_3')]$ · acetone (**4a**·$C_3H_6O$) were determined by X-ray structure analyses. Complex **4** is the first complex that models the unusual 2:1 cyano/carbonyl and dithiolate coordination of the [NiFe] hydrogenase iron site. Complex **4** can be reversibly oxidized electrochemically; chemical oxidation of **4** by $[Fe(Cp)_2PF_6]$, however, led to loss of the CO ligand and yielded only products, which could not be characterized. When dissolved in solvents of increasing proton activity (from $CH_3CN$ to buffered $H_2O$), complex **4** exhibits drastic $\nu$(CO) blue shifts of up to 44 $cm^{-1}$, and relatively small $\nu$(CN) red shifts of approximately 10 $cm^{-1}$. The $\nu$(CO) frequency of **4** in $H_2O$ (1973 $cm^{-1}$) is higher than that of any hydrogenase state (1952 $cm^{-1}$). In addition, the $\nu$(CO) frequency shift of **4** in various solvents is larger than that of [NiFe] hydrogenase in its most reduced or oxidized state. These results demonstrate that complexes modeling properly the $\nu$(CO) frequencies of [NiFe] hydrogenase probably need a $[Ni(thiolate)_2]$ unit. The results also demonstrate that the $\nu$(CO) frequency of $[Fe(CN)_2(CO)$-$(thiolate)_2]$ complexes is more significantly shifted by changing the solvent than the $\nu$(CO) frequency of [NiFe] hydrogenases by coupled-proton and electron-transfer reactions. The "iron-wheel" complex $[Fe_6\{Fe('S_3')_2\}_6]$ (**6**) resulting as a minor by-product from the recrystallization of **2** in boiling toluene could be characterized by X-ray structure analysis.

**Keywords:** carbonyl ligands · cyanide ligands · hydrogenases · iron · S ligands

## Introduction

Hydrogenases are enzymes that are indispensable for the biological energy metabolism by means of catalysis of the reversible redox reaction $H_2 \rightarrow 2H^+ + 2e^-$.[1] [NiFe] hydrogenases are the most common type of these enzymes.[2] X-ray structure determinations[3, 4] in conjunction with IR studies[5, 6] of [NiFe] hydrogenases from several sources have revealed that they contain heterobimetallic active centers in which nickel is linked through two cysteinate bridges to a $[Fe(CN)_2$-(CO)] unit. Scheme 1 depicts the active center of *D. gigas*.

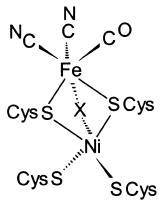


Scheme 1. Schematic structure of the active center in [NiFe] hydrogenase from oxidized *D. gigas* ($X = O^{2-}$ or $OH^-$).[3]

It is to be noted that the nature of the additional X bridge has not been identified with certainty. For the *D. gigas* enzyme, it has been suggested to be a $\mu$-oxo or $\mu$-hydroxo bridge;[3] in the hydrogenases from *D. vulgaris* Miyazaki F[7] or *D. desulfuricans* ATCC 27 774,[8] X possibly is a sulfur atom.

[a] Prof. Dr. D. Sellmann, Dr. F. Geipel, Dr. F. W. Heinemann
Institut für Anorganische Chemie der Universität Erlangen-Nürnberg
Egerlandstrasse 1, 91058 Erlangen (Germany)
Fax: (+49) 9131-8527367
E-mail: sellmann@anorganik.chemie.uni-erlangen.de

[**] Transition Metal Complexes with Sulfur Ligands, Part 152; for Part 151 see: D. Sellmann, N. Blum, F. W. Heinemann, *Z. Naturforsch. B* **2001**, *56*(7), 581.



0947-6539/02/0804-0958 $ 17.50+.50/0 *Chem. Eur. J.* **2002**, *8*, No. 4

The X bridges are assumed to be present only in the (aerobic) deactivated state of the enzymes.

EPR and IR studies of *D. gigas* hydrogenase further showed that the enzyme can exist in numerous different redox states designated, for example, by Ni-A, Ni-B, Ni-SU, Ni-SI, Ni-C, and Ni-R.[5, 9] Each state can be labeled by a different $\nu$(CO) frequency. The $\nu$(CO) frequencies range from 1952 to 1914 $cm^{-1}$ and sometimes differ by only three wavenumbers for two directly related redox states such as Ni-SU (1950 $cm^{-1}$) and Ni-A (1947 $cm^{-1}$).[10]

The EPR studies indicated the nickel site as a redox center and an oxidation state of +II for the iron site in all individual redox states of the enzyme. The $\nu$(CO) frequencies, on the other hand, clearly demonstrated an electronic coupling between the nickel and iron sites. However, a relationship between the redox states and $\nu$(CO) frequencies in the sense that a more reduced state should give rise to lower $\nu$(CO) frequencies does not exist, probably because electron-transfer steps are coupled with proton-transfer steps. Thus low-molecular-weight compounds modeling the binuclear structure of [NiFe] hydrogenases and enabling the study of the effects of electron- and proton-transfer steps in a detailed way are of considerable interest. Such compounds remain unknown in spite of considerable efforts.[11]

Even complexes modeling structure and reactivity features of either the nickel or the iron site are extremely rare. For example, the complex [Ni(NHP*n*Pr$_3$)('S$_3$')] ('S$_3$'$^{2-}$ = bis-(2-mercaptophenyl)sulfide(2 – )) is the only nickel complex that models the distorted sulfur coordination sphere of the nickel site *and* catalyzes the heterolysis of $H_2$.[12] Just as rare are complexes with [Fe(CN)$_2$(CO)] cores. Cyano carbonyl iron complexes with various CN:CO ratios have been known for a considerable time[13] and were recently discovered also in [FeFe] hydrogenase centers;[14] however, the structural motif of two cyano and one carbon monoxide ligand binding to one iron center, is not only without precedence in living matter, but has been found until now in only two complexes. These are [Fe(Cp)(CN)$_2$(CO)]$^-$[15] (Cp = $\eta^5$-cyclopentadienyl) and [Fe(Me$_3$TACN)(CN)$_2$(CO)] (Me$_3$TACN = trimethyltriazacyclononane),[16] and M. Darensbourg et al. could demonstrate that K[Fe(Cp)(CN)$_2$(CO)] and some of its derivatives model remarkably well certain IR spectroscopic features of [NiFe] hydrogenases.[17]

[Fe(CN)$_2$(CO)] complexes with ancillary sulfur ligands have remained unknown. There are a few iron complexes which contain cyano, carbonyl, and sulfur ligands, for example, [Fe(PS3)(CO)(CN)]$^{2-}$ (PS3–H$_3$ = tris(2-phenylthiol)phosphane),[18] [Fe(CO)$_2$(CN)(S$_2$C$_6$H$_4$)]$_2^{2-}$,[19] and [Fe$_2^{II}$(S$_2$C$_3$H$_6$)(CO)$_4$(CN)$_2$]$^{2-}$[20] and are described as models for the active centers of [FeFe] hydrogenases. However, these compounds lack the 2:1 ratio of cyano and carbonyl ligands. In addition the very limited number of these complexes signals the considerable difficulties to synthesize complexes with [Fe(CN)$_2$(CO)(S$_n$)] cores. Here we want to report (NEt$_4$)$_2$-[Fe(CN)$_2$(CO)('S$_3$')], which is the first example of such a complex and resulted from our studies on the coordination chemistry of the [Fe('S$_3$')] fragment.

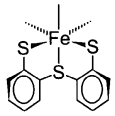

## Results

**Synthesis and structure of [Fe(CO)$_2$('S$_3$')]$_2$ (1)**: All attempts to synthesize characterizable CO complexes with [Fe('S$_3$')] fragments directly from FeCl$_2$·4H$_2$O, 'S$_3$'$^{2-}$, and CO were unsuccessful. In the case of tetra- and pentadentate thiolate thioether ligands, for example, 'S$_4$'$^{2-}$ = 1,2-bis((2-mercaptophenyl)thio)ethanato(2 – ) and 'S$_5$'$^{2-}$ = 2,2'-bis(2-mercaptophenylthio)diethylsulfide(2 – ), this method of preparation yielded the corresponding [Fe(CO)$_2$('S$_4$')] or [Fe(CO)-('S$_5$')] complexes in straightforward reactions.[21] However, when solutions of FeCl$_2$·4H$_2$O in THF or MeOH were treated with 'S$_3$'$^{2-}$ in the presence of CO, immediately black-brown precipitates formed, which were insoluble in all common solvents. These precipitates probably represent polynuclear species related to the "iron-wheel" complex [Fe$_6${Fe('S$_3$')$_2$}$_6$], which is described below.

In the search for [Fe(CO)$_n$('S$_3$')] complexes ($n$ = 2 or 3) we finally found [Fe(CO)$_2$('S$_3$')]$_2$ (**1**). Black-brown crystals of analytically pure [Fe(CO)$_2$('S$_3$')]$_2$ (**1**) formed in a slow reaction according to Equation (1), when 'S$_3$'–H$_2$ and [Fe-(CO)$_3$(MeCOCH=CHPh)] were combined in THF and stored for approximately one week without stirring under ambient conditions. The formation of **1** can be rationalized by a series of reaction steps that include dissociation of the MeCOCH=CHPh ligand, oxidative addition of 'S$_3$'–H$_2$ to the resultant [Fe(CO)$_3$] fragment, reductive elimination of hydride ligands as H$_2$, and release of CO to give [Fe(CO)$_2$('S$_3$')] fragments, which dimerize yielding **1**.

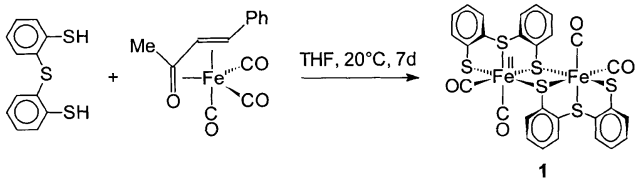


(1)

**1**

Complex **1** crystallized from the reaction solution in about 60% yield. The crystals proved stable in air and extremely sparingly soluble in common organic solvents such that no solution NMR spectra could be recorded. The $\nu$(CO) region of the IR(KBr) spectrum of **1** exhibited only two intensive $\nu$(CO) bands at 2031 and 1991 $cm^{-1}$, and the number of $\nu$(CO) bands indicated that only one diastereomer had formed when the chiral [Fe(CO)$_2$('S$_3$')] fragments dimerized. This was corroborated by X-ray structure crystallography. Figure 1 depicts the molecular structure of **1** and lists selected distances and angles.

Complex **1** possesses crystallographically required centrosymmetry. In **1**, two enantiomeric [Fe(CO)$_2$('S$_3$')] fragments are bridged by thiolate donors of the 'S$_3$' ligand such that the *meso*-diastereomer of [Fe(CO)$_2$('S$_3$')]$_2$ results. Distances and angles show no anomalies. The Fe–S distances lie in the range typical of low-spin Fe$^{II}$ thiolate thioether complexes.[22] It is only to be noted that the Fe–S(thioether) distances (228.0(2) pm) are slightly shorter than the Fe–S(thiolate) distances within one [Fe(CO)$_2$('S$_3$')] fragment (230.3(2) pm; 231.3(2) pm), and that the Fe1–S1a and Fe1a–S1 bridge

  0947-6539/02/0804-0959 $ 17.50+.50/0 

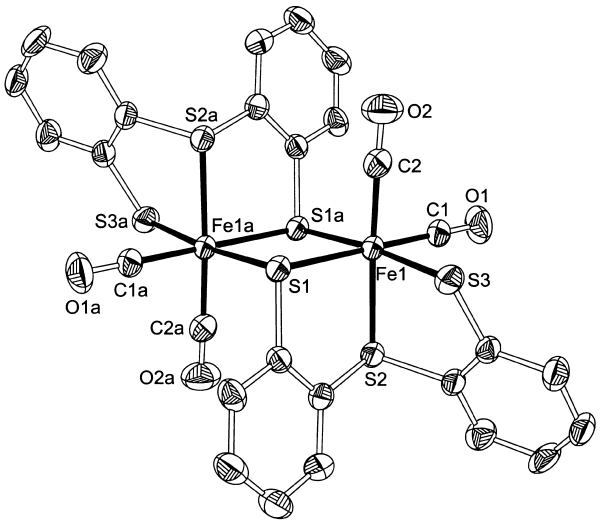


Figure 1. Molecular structure of $[Fe(CO)_2('S_3')]_2$ (**1**) (hydrogen atoms omitted). Selected distances [pm] and angles [°]: Fe1–S1 230.3(2), Fe1–S2 228.0(2), Fe1–S3 231.3(2), Fe1–S1a 233.6(2), Fe1–C1 178.8(6), Fe1–C2 179.8(6), Fe1–Fe1a 345.1(1), S1–S1a 310.1(3), C1–O1 113.2(7), C2–O2 112.6(7), S1–Fe1–C1 177.0(2), S2–Fe1–C2 173.9(2), S3–Fe1–S1a 174.05(6), Fe1–C1–O1 179.7(5), Fe1–C2–O2 178.4(5), S1–Fe1–S1a 83.89(6), S1–Fe1–S2 88.14(6), S1–Fe1–S3 91.82(7), S1–Fe1–C2 91.0(2), C1–Fe1–S1a 93.3(2), C1–Fe1–S2 91.0(2), C1–Fe1–S3 91.0(2), C1–Fe1–C2 90.2(3), S2–Fe1–S3 85.73(6), S2–Fe1–S1a 90.00(6), C2–Fe1–S1a 95.9(2), C2–Fe1–S3 88.2(2), Fe1–S1–Fe1a 96.11(6), a: symmetry code $-x+1, -y, -z+1$.

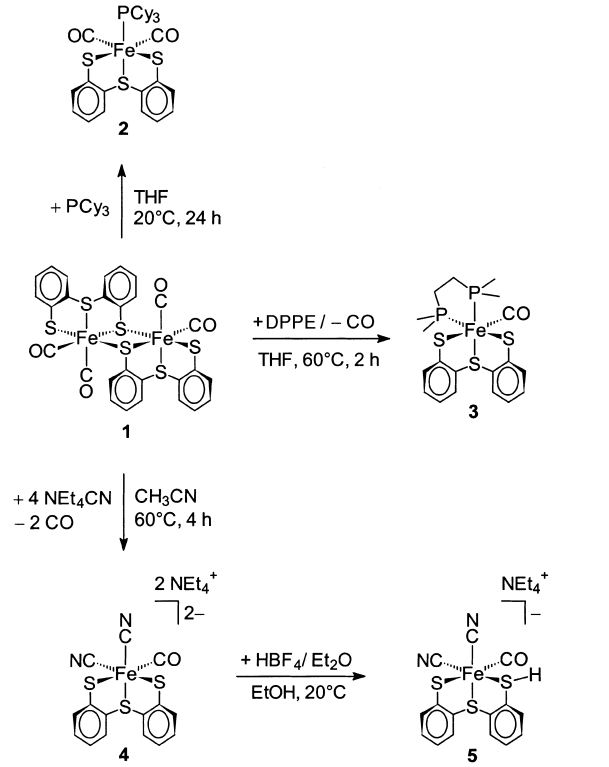


Scheme 2. Syntheses and reactions of $[Fe(L)(L')_2('S_3')]$ complexes (L, L′ = CO, $CN^-$, $PR_3$).

distances are slightly elongated (233.6(2) pm). The most important structural feature of **1** is the facial coordination of the $'S_3'$ ligands. The facial $'S_3'$ coordination results in thiolate donors binding in the *cis*-position to the iron centers, and it contrasts with the $'S_3'$ coordination in distorted planar $[M(L)('S_3')]$ complexes (M = Ni, Pd, Pt, L = monodentate ligands), which have *trans*-S(thiolate) donors.[23] The crystal structure of a second polymorph (**1a**) of **1** has been determined. The corresponding molecular dimensions are in good agreement with those of **1**.

**Reactions of $[Fe(CO)_2('S_3')]_2$ with $PCy_3$, DPPE, and $CN^-$**: In spite of its insolubility, $[Fe(CO)_2('S_3')]_2$ (**1**) proved reactive towards nucleophiles such as $PCy_3$, DPPE, and $NEt_4CN$ and yielded mononuclear complexes of the $[Fe('S_3')]$ fragment. In the course of the respective reactions, black-brown suspensions of **1** in THF slowly turned into dark-red solutions that contained the mononuclear complexes $[Fe(CO)_2(PCy_3)('S_3')]$ (**2**), $[Fe(CO)(dppe)('S_3')]$ (**3**), and $(NEt_4)_2[Fe(CN)_2(CO)('S_3')]$ (**4**) (Scheme 2). These reactions could be monitored by IR solution spectroscopy.

Treatment of **1** with two equivalents of $PCy_3$ in THF yielded $[Fe(CO)_2(PCy_3)('S_3')]$ (**2**). Complex **2**, isolated as red-brown microcrystals, is diamagnetic and proved soluble in THF, $CH_2Cl_2$, acetone, and toluene. The IR spectrum of the reaction solution as well as that of isolated **2** redissolved in THF exhibited in the $\nu$(CO) region only two strong $\nu$(CO) bands at 2015 and 1966 $cm^{-1}$. The number of $\nu$(CO) bands indicated again that stereoselectively only one out of two possible stereoisomers had formed. This could be corroborated by the $^1H$ and $^{13}C$ NMR spectra of **2**. The $^{13}C$ NMR spectrum also enabled us to establish $C_S$ symmetry for **2** as indicated in Scheme 2, because it exhibited only six $^{13}C$ signals for the twelve aromatic C atoms. Accordingly, the $PCy_3$ ligand adopts the position *trans* to the thioether S donor, and the CO ligands both are *trans* to the thiolate S donors. This arrangement of ligands can be rationalized by their π-acceptor or π-donor character: the strong π-acceptor CO ligands prefer positions *trans* to the π-donor thiolates. Dissociation of **1** into two five-coordinate $[Fe(CO)_2('S_3')]$ fragments and their isomerization via square-pyramids and trigonal bipyramids according to Equation (2) enables the CO and L ligands to adopt their favored positions.

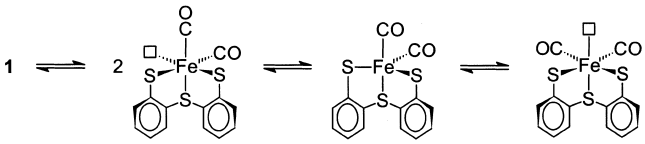


(2)

Treatment of **1** with one equivalent of DPPE yielded $[Fe(CO)(dppe)('S_3')]$ (**3**). In this case, cleavage of the dinuclear **1** is accompanied by CO substitution. Complex **3**, too, is red-brown, diamagnetic, soluble in solvents such as THF, $CH_2Cl_2$, $CH_3CN$, toluene, or acetone, and is produced in a diastereomerically pure form. This was indicated by the IR spectrum showing only one $\nu$(CO) band (1957 $cm^{-1}$ in THF). The $C_1$ symmetry of **3** could be concluded from its $^1H$, $^{13}C$, and $^{31}P$ NMR spectra and was corroborated by the X-ray structure analysis of the toluene solvate $\mathbf{3}\cdot 0.5\,C_7H_8$ grown from solutions in toluene. The stereoselective formation of **3** can



0947-6539/02/0804-0960 $ 17.50+.50/0 *Chem. Eur. J.* **2002**, *8*, No. 4

be rationalized in the same terms as that of **2**: the strong π-acceptor CO ligand prefers a position *trans* to a π-donor thiolate and thus determines the positions left for the two phosphane donors. Figure 2 depicts the molecular structure of **3**·0.5 $C_7H_8$ and lists selected distances and angles.

As in complex **1**, the ′$S_3$′ ligand facially coordinates the Fe center, and the Fe–S distances lie in the usual range. However, it is remarkable that, in spite of different *trans* ligands such as CO and phosphane, the two Fe–S(thiolate) distances (232.9(1), 233.3(1) pm) are identical within the 3σ criterion. The same holds true for the two Fe–P distances. This demonstrates that the [Fe(′$S_3$′)] entity exhibits a considerable structural rigidity towards the electronic influence of different *trans* ligands, although such an influence is evident from the stereoselectivity of the reactions discussed above. As in all complexes with [M(′$S_3$′)] fragments, the Fe–S(thioether) distance (224.5(1) pm) is the shortest Fe–S distance. This can be traced back to the steric requirements of the ′$S_3$′ ligand.[23]

The diastereoselectivity of the reactions leading to **1** as well as to **2** and **3** prompted us to investigate also the reaction of **1** with cyanide ions in order to obtain the [Fe(CN)$_2$(CO)(′$S_3$′)]$^{2-}$ anion. This anion would model the 2:1 ratio of $CN^-$ and CO and the coordination of two cysteine thiolate donors found for the iron site in [NiFe] hydrogenases.

For this purpose, a suspension of **1** in $CH_3CN$ was treated with four equivalents of $NEt_4CN$ at room temperature. In the course of one to two hours, the brown suspension turned into an orange solution. Monitoring the reaction by IR spectroscopy showed that the solution exhibited three ν(CN) bands at 2106, 2084, and 2074 cm$^{-1}$ and three ν(CO) bands at 2033 ,1982, and 1929 cm$^{-1}$ (Figure 3a). These bands could be traced back to the formation of a mixture of the two anions [Fe(CN)(CO)$_2$(′$S_3$′)]$^-$ (designated by °), which forms initially by cleavage of **1**, and [Fe(CN)$_2$(CO)(′$S_3$′)]$^{2-}$ (designated by *), which results from subsequent CO/$CN^-$ exchange. In line with this, gently heating the solution to 60 °C quickly drove the reaction to completion. Then the IR spectrum of the reaction solution exhibited only the ν(CN) and ν(CO) bands of the [Fe(CN)$_2$(CO)(′$S_3$′)]$^{2-}$ anion (Figure 3b).

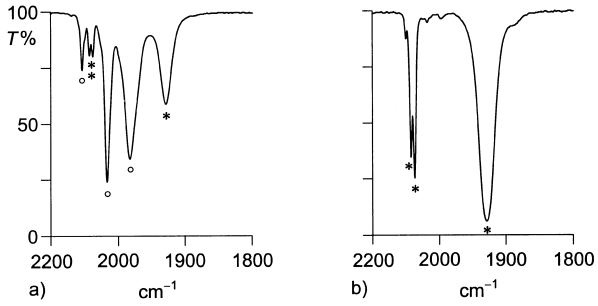


Figure 3. IR monitoring of the reaction between [Fe(CO)$_2$(′$S_3$′)]$_2$ (**1**) and four equivalents of $NEt_4CN$ in $CH_3CN$ at room temperature: a) reaction solution after 40 min containing [Fe(CN)(CO)$_2$(′$S_3$′)]$^-$ (°) and [Fe(CN)$_2$(CO)(′$S_3$′)]$^{2-}$ (*); b) complete formation of [Fe(CN)$_2$(CO)(′$S_3$′)]$^{2-}$ (*) after heating to 60 °C.

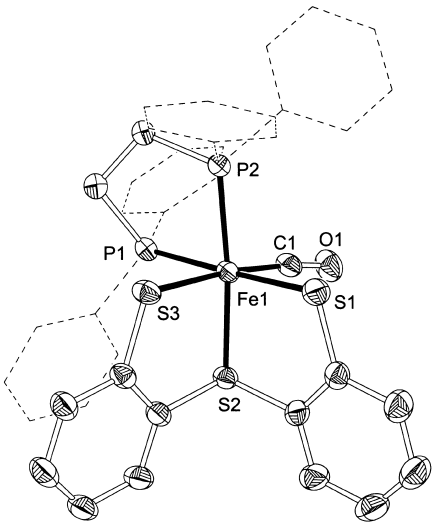


Figure 2. Molecular structure of [Fe(CO)(dppe)(′$S_3$′)]·0.5 toluene (**3**·0.5 $C_7H_8$) (50% probability ellipsoids; hydrogen atoms and solvent molecules omitted; phenyl rings of DPPE are dashed). Selected distances [pm] and angles [°]: Fe1–S1 232.9(1), Fe1–S2 224.5(1), Fe1–S3 233.3(1), Fe1–P1 223.6(1), Fe1–P2 223.7(1), Fe1–C1 175.2(3), C1–O1 115.2(4), S1–Fe1–P1 175.98(3), S2–Fe1–P2 173.58(3), S3–Fe1–C1 173.6(1), S1–Fe1–S2 89.23(3), S1–Fe1–S3 90.36(3), S2–Fe1–S3 88.17(3), S1–Fe1–C1 85.1(1), S1–Fe1–P2 93.02(3), S2–Fe1–C1 87.3(1), S3–Fe1–P1 87.03(3), S2–Fe1–P1 93.74(3), P1–Fe1–P2 83.75(3), P1–Fe1–C1 97.7(1), P2–Fe1–C1 98.9(1).

Workup yielded yellow $(NEt_4)_2$[Fe(CN)$_2$(CO)(′$S_3$′)] (**4**) in approximately 80% yield. Complex **4** was completely characterized by elemental analysis and the common spectroscopic techniques. One ν(CO) IR band and, in particular, seventeen $^{13}C$ signals in the $^{13}C\{^1H\}$ NMR spectrum of **4** arising from one CO, two $CN^-$, twelve aromatic, and two aliphatic C atoms, indicated that the anion of **4** had formed in diastereomerically pure form with $C_1$ symmetry. This could be corroborated by the X-ray structure of $(AsPh_4)_2$[Fe(CN)$_2$(CO)(′$S_3$′)]·acetone (**4a**·$C_3H_6O$), which was obtained by a metathesis from **4** and $AsPh_4Cl$ in acetone. Figure 4 depicts the molecular structure of the [Fe(CN)$_2$(CO)(′$S_3$′)]$^{2-}$ anion in **4a**·$C_3H_6O$ and lists selected distances and angles.

The crystal lattice of **4a**·$C_3H_6O$ consists of discrete cations, anions, and acetone solvate molecules. There are no contacts shorter than the van der Waals radii between the acetone solvate molecules and cations or anions. The C atoms of CO and $CN^-$ ligands and the ′$S_3$′ sulfur donors surround the Fe center pseudo-octahedrally. The thiolate S donors adopt *cis* positions, and the CO ligand is *trans* to one of them. In line with the discussion of the structures of **1** and **3**, the distances and angles of the [Fe(′$S_3$′)] fragment show no anomalies. Although the Fe–CN distances (193.3(9) and 191.2(8) pm) are significantly longer than the Fe–CO distance (177.5(9) pm), in **4**, too, the Fe–S(thiolate) distances *trans* to either a CO or a $CN^-$ ligand (233.5(2) vs. 235.7(2) pm) do not significantly differ and do not reflect a structural *trans* influence of the CO ligand. It is noted that the Fe–CN and Fe–CO distances in [Fe(CN)$_2$(CO)(′$S_3$′)]$^{2-}$ are very similar to those found in [NiFe] hydrogenases isolated from *D. gigas* (Fe–CN (1.9 Å), Fe–CO (1.7 Å), Fe–S (Cys68) (2.2 Å), and Fe–S (Cys533) (2.2 Å)),[3b] *D. vulgaris* Miyazaki F (Fe–CO (1.84–1.93 Å),

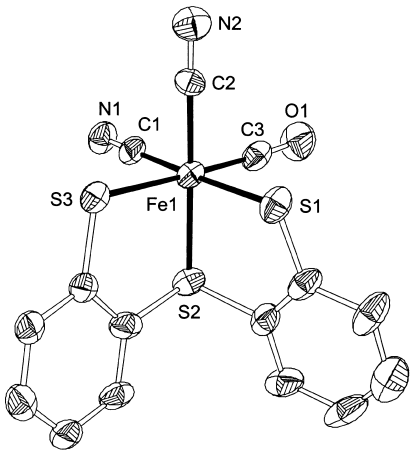


Figure 4. Molecular structure of $[Fe(CN)_2(CO)('S_3')]^{2-}$ in **4a**·acetone (50% probability ellipsoids; hydrogen atoms omitted). Selected distances [pm] and angles [°]: Fe1–S1 233.5(2), Fe1–S2 226.1(2), Fe1–S3 234.7(2), Fe1–C1 193.3(9), Fe1–C2 191.2(8), Fe1–C3 177.5(9), C1–N1 111.6(9), C2–N2 115.3(9), C3–O1 115.9(9), S1–Fe1–C1 176.1(2), S2–Fe1–C2 174.5(2), S3–Fe1–C3 177.6(3), S1–Fe1–S2 87.3(1), S1–Fe1–S3 92.3(1), S2–Fe1–S3 88.3(1), S1–Fe1–C3 87.3(3), S1–Fe1–C2 89.6(2), S2–Fe1–C1 93.1(3), S2–Fe1–C3 94.0(3), S3–Fe1–C1 91.6(2), S3–Fe1–C2 87.3(2), C1–Fe1–C2 90.3(3), C1–Fe1–C3 88.8(3), C2–Fe1–C3 90.4(3), Fe1–C1–N1 177.8(7), Fe1–C2–N2 177.7(8), Fe1–C3–O1 176.3(8).

Fe–S (Cys84) (2.29 Å), and Fe–S (Cys549) (2.36 Å)),[4] and *D. baculatum* (Fe–CN (1.9 Å), Fe–CO (1.9 Å), Fe–S (Cys68) (2.3 Å), and Fe–S (Cys490) (2.3 Å)).[7]

**Chemical properties of $(NEt_4)_2[Fe(CN)_2(CO)('S_3')]$**: In the solid state, complex **4** is relatively stable in air, in solution, however, it is rapidly oxidized by air and decomposes with loss of CO. The solutions of **4** then turn from yellow to dark green. Attempts to oxidize **4** with $[(Cp)_2Fe]PF_6$ in order to determine a redox dependency of the $\nu$(CO) frequency remained unsuccessful and yielded decomposition products only that did not exhibit any $\nu$(CO) bands.

The cyclic voltammogram (CV) of **4** in $CH_3CN$ (Figure 5a) shows two anodic redox processes at $-98$ mV and $+489$ mV (vs. NHE). These redox processes are largely irreversible and

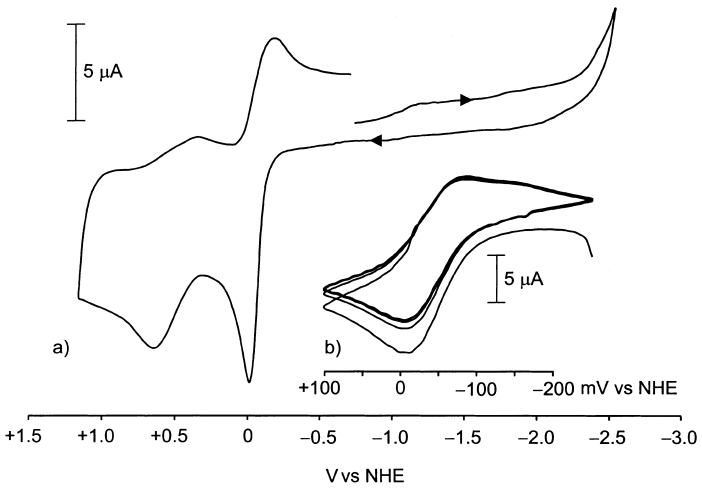


Figure 5. Cyclic voltammogram of $(NEt_4)_2[Fe(CN)_2(CO)('S_3')]$ (**4**) in $CH_3CN$ (0.1 M $[nBu_4N][PF_6]$): a) in the range from $+1.0$ to $-2.5$ V at 250 mV s$^{-1}$; b) from $+0.10$ to $-0.25$ V at 100 mV s$^{-1}$.

thus correspond with the results obtained by the chemical oxidation of **4**. However, the redox process at $-98$ mV becomes quasireversible when the current is reversed at 100 mV (Figure 5b). This redox wave can be assigned to a $Fe^{II}/Fe^{III}$ redox reaction yielding the 17 valence electron complex $[Fe(CN)_2(CO)('S_3')]^-$. Cathodic redox waves could not be observed down to the solvent window ($-2.5$ V for $CH_3CN$).[24]

The good solubility of **4** in $CH_3CN$, MeOH, EtOH, and $H_2O$ permitted the study of the solvent shift of its $\nu$(CO) and $\nu$(CN) bands in different solvents. Table 1 shows that this solvent shift is extremely large for the $\nu$(CO) band which is blue-

Table 1. Comparison of $\nu$(CO)/$\nu$(CN) frequencies [cm$^{-1}$] of $(NEt_4)_2[Fe(CN)_2(CO)('S_3')]$ (**4**), $NEt_4[Fe(CN)_2(CO)('S_3'–H)]$ (**5**), $K[Fe(Cp)(CN)_2(CO)]$, and $H[Fe(Cp)(CN)_2(CO)]$ in different solvents.

| complex | solvent | $\nu$(CO) | $\nu$(CN) |
|---|---|---|---|
| $(NEt_4)_2[Fe(CN)_2(CO)('S_3')]$ (**4**) | KBr | 1924 | 2074 |
| | $CH_3CN$ | 1929 | 2085, 2076 |
| | EtOH | 1959 | 2083, 2072 |
| | MeOH | 1960 | 2085, 2073 |
| | $H_2O$ (pH 7) | 1973 | 2074, 2065 |
| $NEt_4[Fe(CN)_2(CO)('S_3'–H)]$ (**5**) | KBr | 1960 | 2099 |
| $K[Fe(\eta^5\text{-}C_5H_5)(CN)_2(CO)]$[17] | KBr | 1954, 1973 | 2085, 2095 |
| | $CH_3CN$ | 1949 | 2088, 2094 |
| | $H_2O$ | 1979 | 2068, 2083 |
| $H[Fe(\eta^5\text{-}C_5H_5)(CN)_2(CO)]$[17] | KBr | 1991 | 2106, 2135 |
| | $CH_3CN$ | 1988 | 2096, 2107 |
| | $H_2O$ | 1979 | 2068, 2083 |

shifted by 44 cm$^{-1}$ when $CH_3CN$ is replaced by $H_2O$. The $\nu$(CN) bands are much less shifted and they are rather red-shifted decreasing from 2085/2076 cm$^{-1}$ in $CH_3CN$ to 2074/2065 cm$^{-1}$ in $H_2O$.

These shifts can be traced back to the formation of hydrogen bridge bonds between solvent protons and Brønsted-basic thiolate donors in the $[Fe(CN)_2(CO)('S_3')]^{2-}$ anion (Scheme 3). Their strength increases with increasing solvent acidity. The slight red shift of the $\nu$(CN) bands in water indicates that this solvent is also able to form hydrogen bridges to the cyano ligands. When cyano ligands are protonated they acquire isonitrile character, and isonitriles are good $\pi$ acceptors. Thus, the O–H···NC bridges can be expected to withdraw also electron density from the iron centers, and this explains the particularly large $\nu$(CO) blue shift of **4** in water.

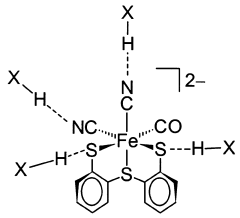


Scheme 3. Strong S···H–X and weak CN···H–X hydrogen bridge bonds between $[Fe(CN)_2(CO)('S_3')]^{2-}$ and solvent protons (X = OEt, OMe, OH).

This interpretation is in line with previous results, which demonstrate that protonation of iron thiolate complexes such as $[Fe(CO)('N_HS_4')]$ ($'N_HS_4'^{2-}$ = 2,2′-bis(2-mercaptophenyl-

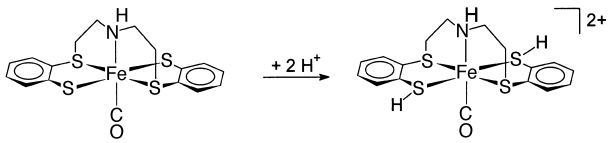


$[Fe(CO)('N_HS_4')]$



0947-6539/02/0804-0962 $ 17.50+.50/0 *Chem. Eur. J.* **2002**, *8*, No. 4

thio)diethylamine(2–))[25] and related species blue shifts their $\nu$(CO) frequencies by approximately 40 cm$^{-1}$ per step of protonation.

In order to corroborate this interpretation we treated a solution of **4** in ethanol with one equivalent of $HBF_4$ in $Et_2O$. Instantaneously a green solid precipitated from the solution. It proved too insoluble for purification by recrystallization; its elemental analysis, however, was compatible with the formation of $(NEt_4)$[Fe(CN)$_2$(CO)($'S_3'$–H)] (**5**), exhibiting one $NEt_4^+$ cation less than **4** and a [$'S_3'$–H]$^-$ ligand as the monoprotonated form of $'S_3'^{2-}$. Complex **5** could be further characterized by its IR(KBr) spectrum showing a band of medium intensity at 2383 cm$^{-1}$, which is assignable to a $\nu$(SH) band. The $\nu$(CO) and $\nu$(CN) bands of **5** appeared at 1960 and 2099 cm$^{-1}$, that is, they both were blue-shifted by 36 and 25 cm$^{-1}$ in comparison with the respective bands of **4** in KBr (1924, 2074 cm$^{-1}$).

The general IR spectroscopic trends observed for **4** in different solvents are very similar to those observed by M. Darensbourg et al. for K[Fe(Cp)(CN)$_2$(CO)] and the respective proton derivative H[Fe(Cp)(CN)$_2$(CO)].[17] For example, **4** as well as K[Fe(Cp)(CN)$_2$(CO)] experience a comparably large $\nu$(CO) shift to higher frequencies when KBr is replaced by $CH_3CN$ or $H_2O$. This is remarkable in so far as in K[Fe(Cp)(CN)$_2$(CO)] only the terminal N atoms of the cyano ligands can act as Brønsted bases, whereas **4** has additional thiolate donors. The most significant difference between **4** and K[Fe(Cp)(CN)$_2$(CO)] certainly is that the $\nu$(CO) frequency always appears approximately 20 cm$^{-1}$ lower in **4** than in K[Fe(Cp)(CN)$_2$(CO)] with one exception: when water is the solvent, the $\nu$(CO) frequencies differ by 6 cm$^{-1}$ only. These effects are certainly due to the different electron-donating capacities of the $C_5H_5^-$ and $'S_3'^{2-}$ ligands, and they also show that water can level electronic differences probably by forming hydrogen bridges of varying numbers and strength with different complexes.

**Formation and molecular structure of [Fe$_6${Fe($'S_3'$)$_2$}$_6$]·8toluene (6·8C$_7$H$_8$)**: The molecular structure of **1** demonstrates the stabilization of coordinatively unsaturated [Fe(CO)$_2$($'S_3'$)] fragments by formation of Fe–S–Fe bridges. Such bridges are also present in [Fe$_6${Fe($'S_3'$)$_2$}$_6$]·8toluene (**6**·8C$_7$H$_8$). This complex formed as a minor by-product when [Fe(CO)$_2$(PCy$_3$)($'S_3'$)] (**2**) was recrystallized from boiling toluene. Complex **6** had not been a target molecule of our investigations, and for this reason, we did not search for a deliberate synthesis. However, the structure of **6**, representing a twelve nuclear "iron wheel", is so unusual that it merits description here. The formation of **6** can be rationalized by a complete dissociation of [Fe(CO)$_2$(PCy$_3$)($'S_3'$)] under harsher conditions (in boiling toluene), in the course of which [Fe($'S_3'$)$_2$]$^{2-}$ and $Fe^{2+}$ ions result which combine to give complex **6**. Figure 6a depicts the molecular structure of **6**·8C$_7$H$_8$ and lists selected distances and angles. Figure 6b depicts one of the six [Fe{Fe($'S_3'$)$_2$}] building units of **6**·8C$_7$H$_8$ showing that a four-coordinate $Fe^{II}$ atom binds to two thiolate donors of one [Fe($'S_3'$)$_2$]$^{2-}$ unit containing a six-coordinate $Fe^{II}$ center. This motif is repeated six times in which four- and six-coordinate $Fe^{II}$ centers alternate leading to the ring structure of **6**.

Three particular points are to be noted.

1) The four-coordinate $Fe^{II}$ centers each bridge two enantiomeric [Fe($'S_3'$)$_2$]$^{2-}$ units.
2) All Fe–S distances lie in the range of Fe–S distances observed in diamagnetic $Fe^{II}$ complexes of polydentate thioether thiolate ligands, for example, [Fe(CO)($'N_HS_4'$)] or [Fe(CO)($'S_5'$)] (vide supra).[26]
3) The Fe–S(thioether) distances in the [Fe($'S_3'$)$_2$] units are particulary short (221 pm). The shortness of these distances is due to the steric requirements of the $'S_3'$ ligands and is typical for all [M($'S_3'$)] complexes (vide supra and refs. [12b] and [23]).

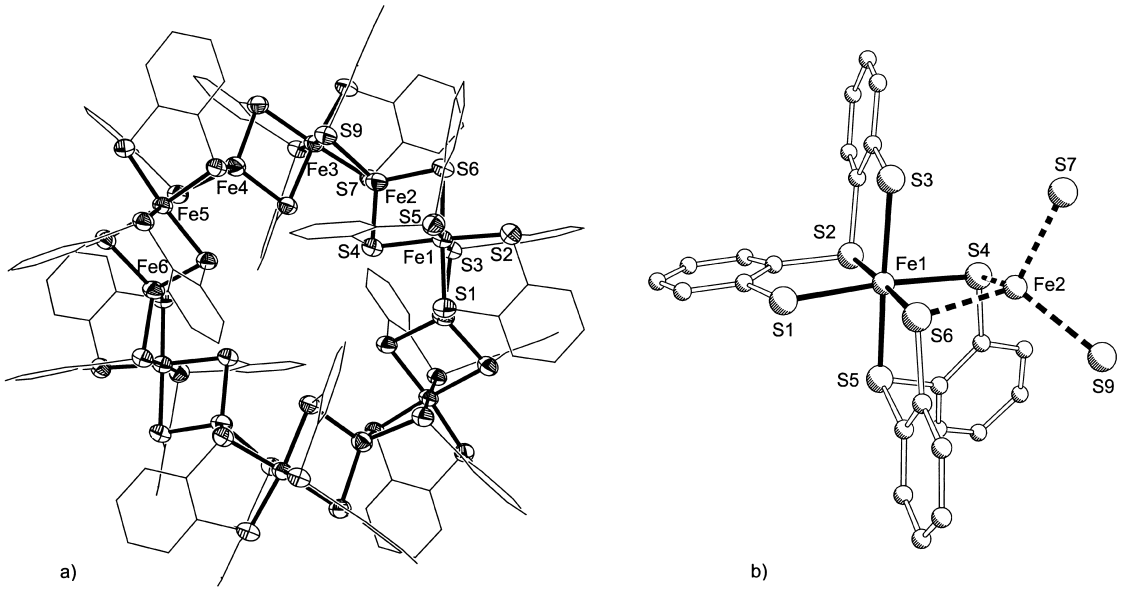


Figure 6. a) Molecular "iron wheel" structure of [Fe$_6${Fe($'S_3'$)$_2$}$_6$] in **6**·8C$_7$H$_8$ (thermal ellipsoids at 50% probability level, hydrogen atoms omitted, phenyl rings lined). Distances [pm]: Fe–S(thiolate) 230.3–233.4, Fe–S(thioether) 221.2–223.6, Fe–Fe 297.5–306.4. Bond angles [°]: *trans* S–Fe$_O$–S 172.9–177.6, *cis* S–Fe$_O$–S 84.6–97.7, S–Fe$_T$–S 96.3–117.9, Fe$_O$–S–Fe$_T$ 79.7–97.4; b) One of the six [Fe{Fe($'S_3'$)$_2$}] units in **6**·8C$_7$H$_8$. Distances [pm]: Fe1–S1 230.5(2), Fe1–S2 221.5(2), Fe1–S3 231.7(2), Fe1–S4 233.4(2), Fe1–S5 221.2(2), Fe1–S6 231.1(2), Fe2–S4 232.3(2), Fe2–S6 231.5(2), Fe2–S7 231.5(2), Fe2–S9 232.2(2).

## Conclusion

In the search for complexes that model the coordination sphere of the iron centers in [NiFe] hydrogenases, in particular the CN:CO ratio of 2:1 and the thiolate coordination, the complex $(NEt_4)_2[Fe(CN)_2(CO)('S_3')]$ (**4**) was found. Entry to the coordination chemistry of $[Fe('S_3')]$ complexes was afforded by the synthesis of $[Fe(CO)_2('S_3')]_2$ (**1**). Treatment of **1** with four equivalents of $NEt_4CN$ yielded **4**. The controlled cleavage of the dinuclear $[Fe(CO)_2('S_3')]_2$ and substitution of exactly one CO group per iron center by $NEt_4CN$ can be traced back to the *trans* influence of thiolate and thioether donors in the $[Fe('S_3')]$ fragment. Such an influence is evidenced by the diastereoselective formation of $[Fe(CO)_2(PCy_3)('S_3')]$ (**2**) and $[Fe(CO)(dppe)('S_3')]$ (**3**) when **1** is treated with mono- or bidentate phosphanes. It is rationalized by the π-donor and π-acceptor properties of thiolate versus thioether ligands. $(NEt_4)_2[Fe(CN)_2(CO)('S_3')]$ (**4**) is, to the best of our knowledge, the first synthetic complex that duplicates the $[Fe(CN)_2(CO)(thiolate)_2]$ coordination of the iron centers in [NiFe] hydrogenases. The third sulfur donor coordinating the Fe center in **4** can be considered to model the oxygen 'X' bridge in *D. gigas* [NiFe] hydrogenases[3] and the sulfur 'X' bridge in hydrogenases from *D. vulgaris* Miyazaki F,[7] or *D. desulfuricans* ATCC 27 774.[8]

After the characterization of **4**, a question of major importance was how the $\nu$(CO) and $\nu$(CN) frequencies of model complexes such as **4** can be used for identifying oxidation states of the enzyme metal centers and redox states of the holoenzymes. The numerous different redox states of *D. gigas* hydrogenase each can be labeled by an individual $\nu$(CO) frequency.[10] However, there is no simple relationship that more reduced states give rise to lower $\nu$(CO) frequencies, probably because in many reaction steps electron- and proton-transfer steps are coupled.

The results obtained with **4** permit the following conclusions.

1) The $\nu$(CO) band of **4** is strongly blue-shifted up to 44 $cm^{-1}$ when **4** is dissolved in solvents of increasing proton activity. The $\nu$(CN) bands are considerably less affected. They are slightly red-shifted, and their red shift is significant only in water (11 $cm^{-1}$).
2) The trends of $\nu$(CO) and $\nu$(CN) shifts of **4** are identical to those observed by M. Darensbourg et al. for $K[Fe(Cp)(CN)_2(CO)]$.[17] However, all three respective bands of **4** appear at lower frequencies than in $K[Fe(Cp)(CN)_2(CO)]$. Most notable is the $\nu$(CO) frequency. In **4**, it is usually 20 $cm^{-1}$ lower than in $K[Fe(Cp)(CN)_2(CO)]$. This $\nu$(CO) difference between **4** and $K[Fe(Cp)(CN)_2(CO)]$ is reduced to only 6 $cm^{-1}$ in $H_2O$, and this indicates that water can strongly level electronic differences in complexes because it is able to form the strongest hydrogen bridges and probably also the largest number of these complex–solvent interactions.
3) The $\nu$(CO) and $\nu$(CN) bands of **4** in KBr (1924, 2074 $cm^{-1}$) or $CH_3CN$ (1929, 2074, 2084 $cm^{-1}$) compare with the frequencies of the Ni-$SI_a$ enzyme state (1932, 2074, 2086 $cm^{-1}$). The Ni-$SI_a$ state is EPR silent, activates $H_2$, and is assumed to exhibit the oxidation state +II for the Ni as well as the Fe center. However, such a comparison is of limited value only because the $\nu$(CO) and $\nu$(CN) frequencies shift to 1973, 2065, and 2074 $cm^{-1}$, when **4** is dissolved in buffered (pH 7) water. In water, the $\nu$(CO) frequency of **4** lies higher than the highest $\nu$(CO) frequency observed for any enzyme state (Ni–C: $\nu$(CO) 1952 $cm^{-1}$).

The $\nu$(CN) frequencies of **4** in $H_2O$ could be correlated best to the Ni-R state of the enzyme ($\nu$(CN): 2059, 2073 $cm^{-1}$). The Ni-R state is the most reduced enzyme state, however, it shows a $\nu$(CO) band at 1936 $cm^{-1}$. Evidently there are no simple relationships between $\nu$(CO) and $\nu$(CN) frequencies.

4) The $\nu$(CO) shift of 44 $cm^{-1}$ of **4** observed when $CH_3CN$ (1929 $cm^{-1}$) is replaced by $H_2O$ (1973 $cm^{-1}$) is larger than that observed for most different enzyme states judging by their different $\nu$(CO) frequencies. These are the Ni-SI ($\nu$(CO): 1914 $cm^{-1}$) and Ni-C states ($\nu$(CO): 1952 $cm^{-1}$). The interconversion of these states requires proton- and electron-transfer reactions. In conclusion, the solvent-dependent $\nu$(CO) shifts of **4** demonstrate that varying exclusively the solvent exerts a larger effect upon the $\nu$(CO) frequencies than coupled electron-proton transfer reactions of the enzyme.

It also has to be stated that investigations of mononuclear iron complexes do not yet suffice to determine unambiguously the different enzyme states with respect to the metal oxidation and protonation states of the active centers, even if these complexes exhibit $[Fe(CN)_2(CO)(S–thiolate)_2]$ cores, which are nearly identical to the iron site in [NiFe] hydrogenases. Evidently, model complexes are needed which practically copy the structure of the active centers. In this context a question of major concern is how binding a $[Ni(SR)_2]$ entity to $[Fe(CN)_2(CO)('S_3')]^{2-}$ cores will affect the $\nu$(CO) frequency. This is part of our current research.

## Experimental Section

**General methods**: Unless noted otherwise, all reactions and spectroscopic measurements were carried out at room temperature under nitrogen by using standard Schlenk techniques. Solvents were dried and distilled before use. As far as possible, reactions were monitored by IR spectroscopy. Buffered $H_2O$ solutions (phosphate buffer, pH 7) were used for recording the IR spectra of aqueous solutions of **4**. Spectra were recorded on the following instruments: IR (KBr discs or $CaF_2$ cuvettes with compensation of the solvent bands): Perkin Elmer 983, 1620 FT IR; NMR: JEOL-JNM-GX 270, EX 270, and Lambda LA 400 with the residual protio-solvent signal used as an internal reference. Chemical shifts are quoted on the $\delta$ scale (downfield shifts are positive) relative to tetramethylsilane ($^1H$, $^{13}C\{^1H\}$ NMR) or 85% $H_3PO_4$ ($^{31}P\{^1H\}$ NMR); mass spectra: JEOL MSTATION 700 spectrometer; elemental analyses: Carlo Erba EA 1106 or 1108 analyzer; cyclic voltammetry: DEA-332 electrochemical analyzer, utilizing a glassy carbon working electrode, platinum reference electrode, and platinum auxiliary electrode. Cyclic voltammograms were obtained from 1.5 mM analyte concentration in $CH_3CN$ by using 0.1M $[nBu_4N][PF_6]$ supporting electrolyte. All potentials were scaled to NHE by using ferrocene ($E_{1/2} = 400$ mV in $CH_3CN$) as internal standard. $NEt_4CN$ and $HBF_4$ (54% in $Et_2O$) were purchased from Fluka and Aldrich. $'S_3'–H_2$ = Bis(2-mercapto-phenyl)sulfide,[23a] $[Fe(CO)_3(MeCOCH{=}CHPh)]$,[27] $Ph_2PCH_2CH_2PPh_2$ = DPPE,[28] and $PCy_3$[29] were prepared by literature methods.

**Syntheses**

**$[Fe(CO)_2('S_3')]_2$ (1)**: Without stirring, a dark green solution of $'S_3'–H_2$ (1.02 g, 3.78 mmol) and $[Fe(CO)_3(MeCOCH{=}CHPh)]$ (1.08 g, 3.78 mmol)



0947-6539/02/0804-0964 $ 17.50+.50/0 *Chem. Eur. J.* **2002**, *8*, No. 4

in THF (50 mL) was stored for one week in a Schlenk tube connected to a gas valve for removing liberated CO and $H_2$. Black-brown crystals of **1** precipitated, were separated, washed with THF, and dried in vacuo. Yield: 905 mg (66%); IR (KBr): $\tilde{\nu}$ = 2031, 1991 cm$^{-1}$ (CO); elemental analysis calcd (%) for $C_{28}H_{16}Fe_2O_4S_6$ (720.49): C 46.68, H 2.24, S 26.70; found: C 46.81, H 2.26, S 26.63.

**[Fe(CO)$_2$(PCy$_3$)('S$_3$')] (2)**: [Fe(CO)$_2$('S$_3$')]$_2$ (**1**) (428 mg, 0.59 mmol) and $PCy_3$ (333 mg, 1.18 mmol) were combined in THF (15 mL). The resulting brown suspension was stirred at room temperature for 24 h to give a dark red solution. It was filtered, and *n*-hexane (ca. 80 mL) was added dropwise. A red-brown solid precipitated, which was separated, washed with *n*-hexane, and dried in vacuo. Yield: 462 mg (61%); $^1$H NMR (269.7 MHz, $CD_2Cl_2$): $\delta$ = 7.56 (d, $J$ = 7.8 Hz, 2H; $C_6H_4$), 7.50 (d, $J$ = 7.8 Hz, 2H; $C_6H_4$), 7.02 (m, 2H; $C_6H_4$), 6.89 (m, 2H; $C_6H_4$), 2.40 – -1.24 (m, 33H; $PC_6H_{11}$); $^{13}$C{$^1$H} NMR (67.8 MHz, $CD_2Cl_2$): $\delta$ = 211.3 (d, $^2J_{PC}$ = 20.1 Hz, CO), 154.0 (d, $^3J_{PC}$ = 7.8 Hz), 136.9, 130.5, 129.6, 129.1, 122.3 ($C_6H_4$), 37.1 (d, $^1J_{PC}$ = 16.8 Hz), 30.0, 27.9 (d, $^2J_{PC}$ = 10.1 Hz), 26.5 ($C_6H_{11}$); $^{31}$P{$^1$H} NMR (161.7 MHz, $CD_2Cl_2$): $\delta$ = 56.71 ($PC_6H_{11}$); IR (KBr): $\tilde{\nu}$ = 2012, 1965 cm$^{-1}$ (CO); MS (FD, $CD_2Cl_2$): $m/z$ (%): 640 [Fe(CO)$_2$(PCy$_3$)('S$_3$')]$^+$; elemental analysis calcd (%) for $C_{32}H_{41}FeO_2PS_3$ (640.68): C 59.99, H 6.45, S 15.01; found: C 59.59, H 7.02, S 14.73.

**[Fe(CO)(dppe)('S$_3$')]·0.5 toluene (3·0.5 C$_7$H$_8$)**: [Fe(CO)$_2$('S$_3$')]$_2$ (**1**) (260 mg, 0.36 mmol) and DPPE (287 mg, 0.72 mmol) were combined in THF (10 mL). The resulting brown suspension was stirred and heated to 60 °C for 1–2 h to give a red solution. The solution was cooled to room temperature and filtered. All volatile components were removed in vacuo to give a red-brown residue. It was redissolved in warm toluene (60 °C, ca. 20 mL) to obtain a saturated solution, which was filtered while warm and stored at room temperature for 24 h and −30 °C for one week. Dark red single crystals formed, which were separated, washed with MeOH, and dried in vacuo. Yield: 358 mg (64%); $^1$H NMR (399.7 MHz, $CD_3CN$): $\delta$ = 7.84–6.40 (m, $C_6H_5$, $C_6H_4$), 3.34 – -2.35 (m, 4H; $Ph_2PC_2H_4PPh_2$), 2.24 (s, $H_3CC_6H_5$); $^{13}$C{$^1$H} NMR (100.4 MHz, $CD_3CN$): $\delta$ = 215.6 (dd, $^2J_{PC}$ = 23.1 Hz, $^2J_{PC}$ = 21.5 Hz, CO), 155.9 (d, $J_{PC}$ = 10.6 Hz), 154.4 (d, $J_{PC}$ = 12.3 Hz), 140.1 (d, $J_{PC}$ = 18.2 Hz), 138.7, 138.2, 135.7 (d, $^1J_{PC}$ = 43.4 Hz), 134.7 (d, $^1J_{PC}$ = 33.0 Hz), 133.0–128.3, 127.8, 126.8 (d, $J_{PC}$ = 9.1 Hz), 125.6, 121.6, 121.2 ($C_6H_5$, $C_6H_4$), 26.3 (dd, $^1J_{PC}$ = 30.1 Hz, $^2J_{PC}$ = 12.8 Hz), 24.7 (dd, $^1J_{PC}$ = 33.8 Hz, $^2J_{PC}$ = 9.9 Hz) ($Ph_2PCH_2CH_2PPh_2$), 20.8 ($CH_3C_6H_5$); $^{31}$P{$^1$H} NMR (161.7 MHz, $CD_3CN$): $\delta$ = 73.4, 64.6 (d, $^2J_{PC}$ = 23.0 Hz, $Ph_2PC_2H_4PPh_2$); IR (KBr): $\tilde{\nu}$ = 1944 cm$^{-1}$ (CO); IR ($CH_3CN$): $\tilde{\nu}$ = 1952 cm$^{-1}$ (CO); MS (FD, THF): $m/z$ (%): 730 [Fe(CO)(dppe)('S$_3$')]$^+$; elemental analysis calcd (%) for **3**·0.5 $C_7H_8$ $C_{42.5}H_{36}FeOP_2S_3$ (776.68): C 65.72, H 4.67, S 12.38; found: C 64.65, H 4.61, S 11.97.

**(NEt$_4$)$_2$[Fe(CN)$_2$(CO)('S$_3$')] (4)**: [Fe(CO)$_2$('S$_3$')]$_2$ (**1**) (718 mg, 1.00 mmol) and $NEt_4CN$ (638 mg, 4.08 mmol) were combined in acetonitrile (40 mL). The resulting brown suspension was stirred and heated to 60 °C for 4 h to give a clear orange solution. Removal of all volatile components in vacuo gave a greenish brown residue, which was extracted with acetone (ca. 60 mL) to yield **4** as a yellow residue. This residue was separated, washed with acetone, and dried in vacuo. Yield: 1.06 g (82%); $^1$H NMR (269.7 MHz, $CD_3CN$): $\delta$ = 7.36 (m, 2H; $C_6H_4$), 7.15 (m, 2H; $C_6H_4$), 6.62 (m, 2H; $C_6H_4$), 6.47 (m, 2H; $C_6H_4$), 3.05 (m, 16H; $NCH_2$), 1.05 (t, 24H; $NCH_2CH_3$); $^{13}$C{$^1$H} NMR (67.8 MHz, $CD_3CN$): $\delta$ = 220.2 (CO), 162.0, 161.5 ($C_6H_4$), 155.6, 149.6 (CN), 142.1, 141.4, 131.8, 131.5, 129.8, 129.6, 127.9, 127.6, 119.8, 119.3 ($C_6H_4$), 53.6 ($NCH_2$), 8.3 ($NCH_2CH_3$); IR (KBr): $\tilde{\nu}$ = 2074 cm$^{-1}$ (CN), 1924 cm$^{-1}$ (CO); IR ($CH_3CN$): $\tilde{\nu}$ = 2085, 2074 cm$^{-1}$ (CN), 1929 cm$^{-1}$ (CO); elemental analysis calcd (%) for $C_{31}H_{48}FeN_4OS_3$ (644.79): C 57.55, H 7.50, N 8.69, S 14.92; found: C 56.94, H 8.30, N 8.90, S 13.78.

**(NEt$_4$)[Fe(CN)$_2$(CO)('S$_3$'–H)] (5)**: $HBF_4$ (50 μL, 363 μmol, in $Et_2O$) was added to a yellow solution (25 mL) of (NEt$_4$)$_2$[Fe(CN)$_2$(CO)('S$_3$')] (**4**) (234 mg, 363 μmol) in EtOH. Instantaneously, a green precipitate formed, and the solution discolored completely. The green precipitate was separated, washed with ethanol, and dried in vacuo. It proved insoluble in all common solvents and could not be recrystallized. The elemental analyses were not satisfactory, however, they clearly indicated the formation of the 1:1 salt. Yield: 180 mg (96%); IR (KBr): $\tilde{\nu}$ = 2383 (SH), 2099 cm$^{-1}$ (CN), 1960 cm$^{-1}$ (CO); elemental analysis calcd (%) for $C_{23}H_{29}FeN_3OS_3$ (515.23): C 53.59, H 5.67, N 8.15, S 18.66; found: C 52.06, H 6.13, N 7.79, S 17.45.

**Crystal structure determinations of [Fe(CO)$_2$('S$_3$')]$_2$ (1), [Fe(CO)(dppe)('S$_3$')]·0.5 toluene (3·0.5 C$_7$H$_8$), (AsPh$_4$)$_2$[Fe(CN)$_2$(CO)('S$_3$')]$_2$·acetone (4a·C$_3$H$_6$O), and [Fe$_6${Fe('S$_3$')$_2$}$_6$]·8 toluene (6·8 C$_7$H$_8$)**: Black-brown rhombs of **1** and dark red blocks of **3**·0.5 $C_7H_8$ were obtained directly from the respective reaction solutions. Brown single crystals of **4a**·$C_3H_6O$ were grown by layering a solution of **4** in acetone with a saturated solution of $AsPh_4Cl$ in acetone at +4 °C. Complex **6**·8 $C_7H_8$ was obtained from a saturated solution of [Fe(CO)$_2$(PCy$_3$)('S$_3$')]$_2$ in toluene (**2**), which had been heated to reflux for one to three minutes and stored for three weeks at room temperature. Complex **2** remained in solution, and black blocks of **6**·8 $C_7H_8$ crystallized in a yield of approximately 5%. Suitable single crystals were sealed in glass capillaries under $N_2$. Data were collected on the following diffractometers: Siemens P4 (**1**, **3**·0.5 $C_7H_8$, **4a**·$C_2H_6O$) and

Table 2. Selected crystallographic data for [Fe(CO)$_2$('S$_3$')]$_2$ (**1**), [Fe(CO)(dppe)('S$_3$')]·0.5 toluene (**3**·0.5 $C_7H_8$), (AsPh$_4$)$_2$[Fe(CN)$_2$(CO)('S$_3$')]$_2$·acetone (**4a**·$C_3H_6O$), and [Fe$_6${Fe('S$_3$')$_2$}$_6$]·8 toluene (**6**·8 $C_7H_8$).

| | **1** | **3**·0.5 $C_7H_8$ | **4a**·$C_2H_6O$ | **6**·8 $C_7H_8$ |
|---|---|---|---|---|
| formula | $C_{28}H_{16}Fe_2O_4S_6$ | $C_{42.5}H_{36}FeOP_2S_3$ | $C_{66}H_{54}As_2FeN_2O_2S_3$ | $C_{200}H_{160}Fe_{12}S_{36}$ |
| $M_r$ [g mol$^{-1}$] | 720.49 | 776.68 | 1208.98 | 4387.64 |
| $T$ [K] | 295(2) | 200(2) | 210(2) | 173(2) |
| crystal system | triclinic | monoclinic | triclinic | triclinic |
| space group | $P\bar{1}$ | $C2/c$ | $P\bar{1}$ | $P\bar{1}$ |
| $a$ [pm] | 767.8(3) | 2843.6(6) | 1018.7(1) | 1709.1(1) |
| $b$ [pm] | 780.7(2) | 1445.7(3) | 1245.5(2) | 1823.1(1) |
| $c$ [pm] | 1236.2(3) | 2215.6(3) | 2304.8(5) | 1881.0(1) |
| $\alpha$ [°] | 79.99(2) | 90 | 79.73(2) | 111.245(3) |
| $\beta$ [°] | 80.82(3) | 125.61(1) | 81.31(2) | 115.088(2) |
| $\gamma$ [°] | 72.36(2) | 90 | 78.71(1) | 96.527(3) |
| $V$ [nm$^3$] | 0.6909(4) | 7.41(1) | 2.8012(8) | 4.6926(5) |
| $Z$ | 1 | 8 | 2 | 1 |
| $\rho_{calcd}$ [g cm$^{-3}$] | 1.732 | 1.393 | 1.433 | 1.553 |
| $\mu$ [mm$^{-1}$] | 1.539 | 0.697 | 1.601 | 1.352 |
| crystal size [mm] | 0.24 × 0.12 × 0.10 | 0.52 × 0.44 × 0.40 | 0.30 × 0.20 × 0.18 | 0.42 × 0.18 × 0.10 |
| $T_{min}/T_{max}$ | 0.654/0.788 | – | 0.398/0.487 | – |
| 2$\theta$ range [°] | 5.5–54.0 | 3.5–54.0 | 3.5–50.0 | 4.6–49.5 |
| measured ref. | 3697 | 9286 | 11645 | 27554 |
| unique ref. | 3011 | 8097 | 9824 | 15701 |
| observed ref. | 1935 | 5715 | 5345 | 10273 |
| parameters | 206 | 545 | 699 | 1127 |
| $R1$[a]; $wR2$ [%] | 5.58; 14.23 | 4.54; 11.24 | 6.70; 14.86 | 6.49; 19.07 |

[a] [$I > 2\sigma(I)$].

Nonius Kappa CCD ($\mathbf{6}\cdot 8C_7H_8$),[30] by using $Mo_{K\alpha}$ radiation ($\lambda =$ 71.073 pm), a graphite monochromator, and $\omega$-scan technique. Selected crystallographic data are listed in Table 2.[31] The crystallographic data of a second polymorph of **1** are not included in Table 2 but have been deposited with the CCDC-168523 (**1a**).[31] For **1** and $\mathbf{4a}\cdot C_3H_6O$, an absorption correction was applied on the basis of $\psi$ scans. All structures were solved by direct methods and refined by full-matrix least-squares procedures on $F^2$.[32] All non-hydrogen atoms were refined anisotropically. The positions of the hydrogen atoms in **1**, $\mathbf{3}\cdot 0.5C_7H_8$, and $\mathbf{4a}\cdot C_3H_6O$ were taken from a difference Fourier synthesis. For **1** and $\mathbf{3}\cdot 0.5C_7H_8$, their positional parameters were refined with fixed common isotropic displacement parameters. For $\mathbf{4a}\cdot C_3H_6O$ both the positional parameters and a common isotropic displacement parameter were kept fixed during the refinement. The hydrogen atoms in $\mathbf{6}\cdot 8C_7H_8$ and of the solvent molecule in $\mathbf{3}\cdot 0.5C_7H_8$ were geometrically positioned with isotropic displacement parameters fixed at 1.2 or 1.5 times the $U$(eq) of the adjacent carbon atom. No hydrogen atoms were introduced for the disordered solvate molecule in $\mathbf{4a}\cdot C_3H_6O$. In the structure of $\mathbf{6}\cdot 8C_7H_8$ two of the eight toluene molecules are disordered.

## Acknowledgements

Support of these investigations by the Deutsche Forschungsgemeinschaft, Sonderforschungsbereich 583 "Redoxaktive Metallkomplexe", and Fonds der Chemischen Industrie is gratefully acknowledged.

[1] a) R. Cammack, *Nature* **1999**, *397*, 214; b) M. W. W. Adams, E. I. Stiefel, *Science* **1998**, *282*, 1842; c) R. K. Thauer, A. R. Klein, G. C. Hartmann, *Chem. Rev.* **1996**, *96*(7), 3031; d) S. P. J. Albracht, *Biochim. Biophys. Acta* **1994**, *1188*, 167.

[2] a) M. Frey, *Struct. Bond.* **1998**, *90*, 97; b) J. C. Fontecilla-Camps, *Struct. Bond.* **1998**, *91*, 1; c) M. J. Maroney, G. Davidson, Ch. B. Allan, J. Figlar, *Struct. Bond.* **1998**, *92*, 2.

[3] a) A. Volbeda, M. H. Charon, C. Piras, E. C. Hatchikian, M. Frey, J. C. Fontecilla-Camps, *Nature* **1995**, *373*, 580; b) A. Volbeda, E. Garcin, C. Piras, A. L. de Lacey, V. M. Fernandes, E. C. Hatchikian, M. Frey, J. C. Fontecilla-Camps, *J. Am. Chem. Soc.* **1996**, *118*, 12989.

[4] E. Garcin, E. C. Hatchikian, A. Volbeda, M. Frey, J. C. Fontecilla-Camps, *Structure* **1999**, *7*, 557.

[5] a) A. L. de Lacey, E. C. Hatchikian, A. Volbeda, M. Frey, J. C. Fontecilla-Camps, V. M. Fernandez, *J. Am. Chem. Soc.* **1997**, *119*, 7181; b) R. P. Happe, W. Roseboom, K. A. Bagley, A. J. Pierik, S. P. J. Albracht, *Nature* **1997**, *385*, 126.

[6] a) K. A. Bagley, E. C. Duin, W. Roseboom, S. P. J. Albracht, W. H. Woodruff, *Biochemistry* **1995**, *34*, 5527; b) T. M. Van der Spek, A. F. Arendsen, R. P. Happe, S. Yun, K. A. Bagley, D. J. Stufkens, W. R. Hagen, S. P. J. Albracht, *Eur. J. Biochem.* **1996**, *237*, 629.

[7] a) Y. Higuchi, T. Yagi, N. Yasuoka, *Structure* **1997**, *5*, 1671; b) Y. Higuchi, H. Ogata, K. Miki, N. Yasuoka, T. Yagi, *Structure* **1999**, *7*, 549.

[8] P. M. Matias, C. M. Soares, L. M. Saraiva, R. Coelho, J. Morais, J. LeGall, M. A. Carrondo, *J. Biol. Inorg. Chem.* **2001**, *6*, 63.

[9] F. Dole, A. Fournel, V. Magro, E. C. Hatchikian, P. Betrand, B. Guigliarelli, *Biochemistry* **1997**, *36*, 7847.

[10] M. J. Maroney, P. A. Bryngelson, *J. Biol. Inorg. Chem.* **2001**, *6*, 63.

[11] a) M. Y. Darensbourg, E. J. Lyon, J. J. Smee, *Coord. Chem. Rev.* **2000**, *206–207*, 553; b) G. J. Colpas, R. O. Day, M. J. Maroney, *Inorg. Chem.* **1992**, *31*, 5053; c) F. Osterloh, W. Saak, D. Haase, S. Pohl, *Chem. Commun.* **1996**, 777; d) C.-H. Lai, J. H. Reibenspies, M. Y. Darensbourg, *Angew. Chem.* **1996**, *108*, 2551; *Angew. Chem. Int. Ed. Engl.* **1996**, *35*, 2390; e) F. Osterloh, W. Saak, D. Haase, S. Pohl, *Chem. Commun.* **1997**, 979; f) E. Bouwman, R. K. Henderson, A. L. Spek, J. Reedijk, *Eur. J. Inorg. Chem.* **1999**, *4*, 217; g) S. C. Davies, D. J. Evans, D. L. Hughes, S. Longhurst, J. R. Sanders, *Chem. Commun.* **1999**, 1935; h) G. Steinfeld, B. Kersting, *Chem. Commun.* **2000**, 205; i) W.-F. Liaw, C.-Y. Chiang, G.-H. Lee, S.-M. Peng, C.-H. Lai, M. Y. Darensbourg, *Inorg. Chem.* **2000**, *39*, 480.

[12] a) D. Sellmann, F. Geipel, M. Moll, *Angew. Chem.* **2000**, *112*, 570; *Angew. Chem. Int. Ed.* **2000**, *39*, 561; b) D. Sellmann, F. Geipel, F. W. Heinemann, *Eur. J. Inorg. Chem.* **2000**, 59.

[13] a) S. A. Goldfield, K. N. Raymond, *Inorg. Chem.* **1974**, *13*, 770; b) M. Moll, H. Behrens, W. Popp, *Z. Anorg. Allg. Chem.* **1979**, *458*, 202; c) M. Y. Darensbourg, H. L. C. Barros, *Inorg. Chem.* **1979**, *18*, 3286; d) G. Reichenbach, G. Bellachioma, *J. Chem. Soc. Dalton Trans.* **1987**, *3*, 519.

[14] a) J. W. Peters, W. N. Lanzilotta, B. J. Lemon, L. C. Seefeldt, *Science* **1998**, *282*, 1853; b) Y. Nicolet, C. Piras, P. Legrand, E. C. Hatchikian, J. C. Fontecilla-Camps, *Structure* **1999**, *7*, 13.

[15] a) C. E. Coffey, *Inorg. Nucl. Chem.* **1963**, *25*, 179; b) D. J. Darensbourg, J. H. Reibenspies, C.-H. Lai, W-Z. Lee, M. Y. Darensbourg, *J. Am. Chem. Soc.* **1997**, *119*, 7903.

[16] A. C. Moreland, T. B. Rauchfuss, *Inorg. Chem.* **2000**, *39*, 3029.

[17] a) C.-H. Lai, W.-Z. Lee, M. L. Miller, J. H. Reibenspies, D. J. Darensbourg, M. Y. Darensbourg, *J. Am. Chem. Soc.* **1998**, *120*, 10103.

[18] H.-F. Hsu, S. A. Koch, C. V. Popescu, E. Münck, *J. Am. Chem. Soc.* **1997**, *119*, 8371.

[19] W-F. Liaw, N-H. Lee, C-H. Chen, C-M. Lee, G-H. Lee, S-M. Peng, *J. Am. Chem. Soc.* **2000**, *122*, 488.

[20] a) E. J. Lyon, I. P. Georgakaki, J. H. Reibenspies, M. Y. Darensbourg, *Angew. Chem.* **1999**, *111*, 3373; *Angew. Chem. Int. Ed.* **1999**, *38*, 3178; b) M. Schmidt, S. M. Contakes, T. B. Rauchfuss, *J. Am. Chem. Soc.* **1999**, *121*, 9736; c) A. Le Cloires, S. P. Best, S. Borg, S. C. Davies, D. L. Hughes, C. J. Pickett, *Chem. Commun.* **1999**, 2285.

[21] a) D. Sellmann, H. E. Jonk, H. R. Pfeil, G. Huttner, J. von Seyerl, *J. Organomet. Chem.* **1980**, *191*, 171; b) D. Sellmann, U. Kleine-Kleffmann, *J. Organomet. Chem.* **1983**, *247*, 307.

[22] D. Sellmann, R. Weiss, F. Knoch, G. Ritter, J. Dengler, *Inorg. Chem.* **1990**, *29*, 4107.

[23] a) D. Sellmann, D. Häußinger, F. W. Heinemann, *Eur. J. Inorg. Chem.* **1999**, 1715; b) D. Sellmann, F. Geipel, F. W. Heinemann, *Eur. J. Inorg. Chem.* **2000**, 271.

[24] A. J. Bard, L. R. Faulkner, *Electrochemical Methods*, Wiley, New York, **1980**.

[25] a) D. Sellmann, T. Becker, F. Knoch, *Chem. Eur. J.* **1996**, *2*, 1092; b) D. Sellmann, G. Mahr, F. Knoch, M. Moll, *Inorg. Chim. Acta* **1994**, *224*, 45.

[26] a) D. Sellmann, H. Kunstmann, F. Knoch, M. Moll, *Inorg. Chem.* **1988**, *27*, 4183; b) D. Sellmann, G. Binker, M. Moll, E. Herdtweck, *J. Organomet. Chem.* **1987**, *327*, 403.

[27] A. J. P. Domingos, J. A. S. Howell, B. F. G. Johnson, J. Lewis, *Inorg. Synth.* **1990**, *28*, 52.

[28] W. Hewertson, H. R. Watson, *J. Chem. Soc.* **1962**, 1490.

[29] K. Issleib, A. Brack, *Z. Anorg. Allg. Chem.* **1954**, *277*, 258.

[30] We thank Dr. F. Hampel for X-ray data measurements of $[Fe_6\{Fe(^tS_3')_2\}_6]\cdot 8$toluene ($\mathbf{6}\cdot 8C_7H_8$).

[31] Crystallographic data (excluding structure factors) for the structures reported in this paper have been deposited with the Cambridge Crystallographic Data Centre as supplementary publication nos. CCDC-168522 (**1**), -168523 (**1a**), -168524 ($\mathbf{3}\cdot 0.5C_7H_8$), -168525 ($\mathbf{4a}\cdot C_3H_6O$), and -168526 ($\mathbf{6}\cdot 8C_7H_8$). Copies of the data can be obtained free of charge on application to CCDC, 12 Union Road, Cambridge CB2 1EZ, UK (fax: (+44) 1223-336-033; e-mail: deposit@ccdc.cam.ac.uk).

[32] SHELXTL NT 5.10, Bruker AXS, Inc., Madison, WI, **1998**; or Nonius Collect/HKL, **1999**.

Received: August 16, 2001 [F3495]

  